JACS
JOURNAL OF THE AMERICAN CHEMICAL SOCIETY
Article
pubs.acs.org/JACS

Facile C_{sp^2}–C_{sp^2} Bond Cleavage in Oxalic Acid-Derived Radicals

Robert W. Molt, Jr.,[†] Alison M. Lecher,[‡] Timothy Clark,[§,∥] Rodney J. Bartlett,[‡] and Nigel G. J. Richards*[,†]

[†]Department of Chemistry and Chemical Biology, Indiana University–Purdue University , Indianapolis, Indiana 46202, United States
[‡]Quantum Theory Project, Department of Chemistry, University of Florida, Gainesville, Florida 32611, United States
[§]Computer-Chemie-Centrum and Interdisciplinary Center for Molecular Materials, Department of Chemie und Pharmazie, Friedrich-Alexander-Universität Erlangen-Nürnberg, 91052 Erlangen, Germany
[∥]Centre for Molecular Design, University of Portsmouth, Portsmouth, PO1 2DY, United Kingdom

Supporting Information

ABSTRACT: Oxalate decarboxylase (OxDC) catalyzes the Mn-dependent conversion of the oxalate monoanion into CO_2 and formate. Many questions remain about the catalytic mechanism of OxDC although it has been proposed that the reaction proceeds via substrate-based radical intermediates. Using coupled cluster theory combined with implicit solvation models we have examined the effects of radical formation on the structure and reactivity of oxalic acid-derived radicals in aqueous solution. Our results show that the calculated solution-phase free-energy barrier for C–C bond cleavage to form CO_2 is decreased from 34.2 kcal/mol for oxalic acid to only 9.3 kcal/mol and a maximum of 3.5 kcal/mol for the cationic and neutral oxalic acid-derived radicals, respectively. These studies also show that the C–C σ bonding orbital of the radical cation contains only a single electron, giving rise to an elongated C–C bond distance of 1.7 Å; a similar lengthening of the C–C bond is not observed for the neutral radical. This study provides new chemical insights into the structure and stability of plausible intermediates in the catalytic mechanism of OxDC, and suggests that removal of an electron to form a radical (with or without the concomitant loss of a proton) may be a general strategy for cleaving the unreactive C–C bonds between adjacent sp^2-hybridized carbon atoms.

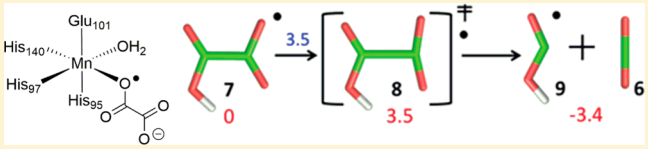

INTRODUCTION

Oxalate decarboxylase (OxDC) is an enzyme found in fungi and some bacteria.[1] The physiological function of OxDC remains ill-defined, although it has been reported that the gene encoding OxDC in *Bacillus subtilis* is involved in the process of sporulation.[2] This enzyme is of considerable mechanistic interest because it catalyzes the conversion of oxalate into CO_2 and formate by cleaving the C–C bond between two adjacent sp^2-hybridized carbon atoms.[3] Recent kinetic studies have shown that OxDC decreases the C–C bond cleavage barrier to approximately 13 kcal/mol under steady-state conditions[3a] from an estimated value of 33 kcal/mol for the uncatalyzed reaction.[4] Although substantial progress has been made in identifying functionally important active site residues,[3,5] the details of the catalytic mechanism by which OxDC facilitates C–C bond breaking remain poorly understood. Most mechanistic proposals (based on heavy-atom isotope effect measurements) postulate that the function of the transition metal center is to generate a Mn-bound oxalate radical in a step prior to decarboxylation.[3a] Efforts to validate these proposals using either QM/MM simulations[6] or quantum mechanical (QM) calculations on active site models[7] are precluded by the current absence of experimental information on a number of aspects, including Mn oxidation and spin state in the active form of the enzyme, the role of dioxygen during catalytic turnover, and the mode by which oxalate coordinates the metal center. On the other hand, spin trapping studies have supported the formation of a formyl radical anion during turnover,[3d] which is consistent with the idea that decarboxylation takes place from an oxalate-derived radical. In an effort to explore the energetic consequences for C–C bond cleavage in such a radical, we have performed the first set of high-level QM calculations that explore the effects of radical formation on the structure and reactivity of oxalic acid in aqueous solution. Our studies clearly show that removing an electron from oxalic acid, with or without concomitant deprotonation, does indeed substantially decrease the barrier to decarboxylation. In addition, we have uncovered unexpected structural differences between the neutral and cationic radicals derived from oxalic acid, which can be attributed to the presence of a one-electron C–C bond in the radical cation. Not only do these QM calculations provide the first insights into the electronic structure of oxalic acid-derived radicals but they also provide additional quantitative evidence for the hypothesis that catalysis in OxDC proceeds via decarboxylation of a substrate-derived radical.

RESULTS AND DISCUSSION

QM calculations were performed to model the energetics of C–C bond cleavage in oxalic acid **1**, the neutral radical **7**, and the radical cation **10** (Figure 1). We note that radical **7**

Received: October 16, 2014
Published: February 21, 2015

DOI: 10.1021/ja510666r
J. Am. Chem. Soc. 2015, 137, 3248–3252

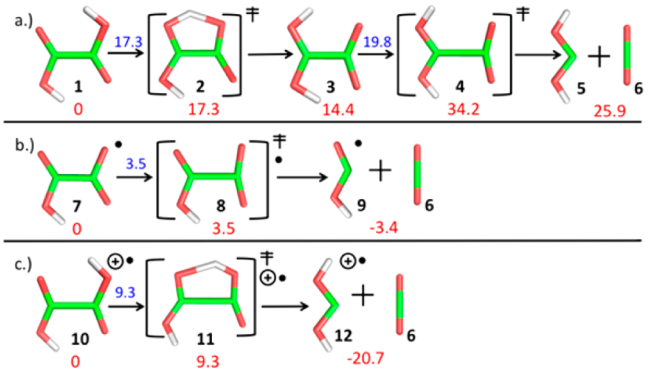

Figure 1. Model reaction pathways for C−C bond cleavage in (a) oxalic acid **1**, (b) the neutral radical **7**, and (c) the radical cation **10**. Calculated solution-phase free energies (kcal/mol) relative to reactant, and activation free energies for each step are shown in red and blue font, respectively.

corresponds to the hypothetical species in the OxDC-catalyzed reaction that would be generated by proton-coupled electron transfer, whereas **10** serves as a model for C−C bond cleavage in the substrate if electron transfer were to take place *without* concomitant removal of a proton. Oxalic acid **1** was initially chosen as a reference system in order to (i) validate our computational strategy and (ii) elucidate changes in bonding and energetics resulting from removal of an electron.

The structures of compounds **1**, **7**, and **10**, together with relevant transition states and intermediates, were obtained in both the gas phase and solution. Unless otherwise noted in the text, optimized geometries and harmonic vibrational frequencies were calculated using the SMD implicit solvation model[8] combined with the M06 functional[9] and cc-pVTZ basis set.[10] This solvation model was chosen because of its strong performance when used with M06; to ensure that the calculated structures were of high quality, however, we employed a larger basis set than those used in previous validation studies.[9,11] Free energies were obtained using gas-phase complete-basis-set (CBS) extrapolated[12] CCSD(T) energies[13] combined with solvation free energies and partition functions for entropy and enthalpy calculated using SMD/M06/cc-pVTZ. Gas phase energies computed with CCSD(T)/CBS are accurate to approximately 1 kcal/mol;[10] we estimate that solvation free energies are accurate to within 3−4 kcal/mol on the basis of blind trials.[11] We note that any single-reference system is compellingly described by using CCSD(T)/cc-pVTZ and CCSD(T)/CBS to obtain gas phase geometries and energies, respectively. In validation studies, all gas phase CCSD(T)/cc-pVTZ bond lengths were within 0.01 Å of those obtained using the M06/SMD description. All calculations were performed using the GAMESS,[14] ACES2,[15] and ACES3[16] software packages.

Effects of Radical Formation on the Energetics of Decarboxylation. We investigated the energetics of possible mechanisms for the uncatalyzed decarboxylation of model compounds **1**, **7**, and **10** with the goal of obtaining a quantitative understanding of how the activation energy for C−C bond cleavage might be reduced in the radical species derived from neutral oxalic acid **1**. Although the gas-phase decomposition of neutral oxalic acid has been studied experimentally and computationally prior to our work,[17] the calculations reported herein provide aqueous free energies rather than the gas phase internal energies computed in previous reports. These authors did not examine the properties of oxalic acid-derived radicals. We performed calculations for all rotameric forms of the three model compounds but discuss only the results for the most stable rotamer of each structure here for simplicity (Figure 1). The barriers computed for alternate rotamers of **1** and **10**, which are generally only 1−2 kcal/mol higher in energy than those discussed below, are only marginally different and do not change the conclusion of this study (see Figure S1 in Supporting Information).[18]

The experimental value[4] for the uncatalyzed conversion of oxalic acid **1** to formate and CO_2 was used to validate our computational strategy. Thus, solution-phase free energy barriers for initial proton transfer and subsequent C−C bond cleavage of **1** were computed to be 17.7 and 19.8 kcal/mol, respectively, giving a total barrier of 34.2 kcal/mol for the reaction (Figure 1). This calculated value is in reasonable agreement with the experimental estimate of 33 kcal/mol.[4] The inclusion of solvation and thermal effects was essential in reproducing experimental measurements because the barrier for this decarboxylation in the gas-phase was calculated to be only ∼25 kcal/mol. We note that exhaustive efforts to locate a transition state for C−C bond cleavage in **1** for a pathway involving concerted proton transfer and decarboxylation failed; the final structure always corresponded to a stationary point with two imaginary harmonic vibrational modes (each corresponding to one of the sequential steps). Given that it has been proposed that OxDC binds the substrate as the monoanion,[3a] we also investigated the barrier for decarboxylation from this species and determined it to be approximately 50 kcal/mol (see Supporting Information).

We next examined the barrier to C−C bond cleavage in the neutral radical **7**, which has been proposed to be an intermediate in the OxDC-catalyzed reaction.[3a] This required, however, minor modifications to our standard computational protocol because M06/SMD density functional calculations predicted this radical to be an unambiguous van der Waals complex with a C−C distance of 2.2 Å and an electronic dissociation barrier of less than 1 kcal/mol. We note that the neutral radical **7** exists as a stationary state in the gas phase (∼1.54 Å C−C bond length) in CCSD and CCSD(T) calculations using cc-pVTZ bases, and the gas phase M06 is comparable, but not within the SMD model. In contrast, calculations using M06-2X,[7] CAM-B3LYP,[19] and M11,[20] density functionals all gave solution-phase structures for **7** containing a standard covalent C−C bond. We therefore used the geometry of **7** obtained by M06-2X/SMD optimization in subsequent calculations. This choice allowed us to obtain a maximal upper bound of the decarboxylation barrier. Decarboxylation from the van der Waals complex would presumably give an even lower barrier. However, for comparing structural aspects, the CCSD structure shown in supplemental information is used. After obtaining the transition state **8** for decarboxylation, the suggestion that OxDC catalyzes C−C bond cleavage by generating radical intermediates was supported by a reduction in the calculated free energy barrier from 34.2 to 3.5 kcal/mol (Figure 1). This barrier for the decarboxylation of the neutral radical **7**, which likely represents an upper-bound estimate, is consistent with the failure of efforts to observe the putative, enzyme-bound, neutral doublet of oxalate using EPR methods.[21] Similar reductions in activation energy barriers for C−C bond cleavage have been reported for carboxyloxy radicals,[22] including those formed during the Kolbe reaction.[23]

DOI: 10.1021/ja510666r
J. Am. Chem. Soc. 2015, 137, 3248−3252

Lastly, we determined the barrier for decarboxylation of the radical cation **10** (Figure 1). In searching for a two-step decomposition mechanism, however, we observed that **10** forms CO_2 via a concerted (simultaneous proton transfer and C−C bond cleavage) rather than a sequential (proton transfer then carbon−carbon cleavage) mechanism. The calculated activation free energy for C−C bond cleavage in the radical cation **10** (9.3 kcal/mol) was again found to be markedly lower than that computed for oxalic acid **1**. In this case, care had to be taken to ensure proper convergence of the reference wave function for transition state **11**, which exhibited wave function instabilities. The higher barrier to decarboxylation for radical cation **10** relative to that computed for the neutral radical **7** likely arises from two factors. First, two bonds have to be broken in the decarboxylation transition state **11** compared to only one in **8** (Figure 1). In addition, formation of transition state **11** from the radical cation reduces the dipole moment of the system, which has the effect of reducing the energetic contribution of the solvation potential to lowering the free energy barrier.

Structural Studies of Radicals Derived from Oxalic Acid. In seeking to understand how the electronic structure of the radicals **7** and **10** might differentially lower the barrier to decarboxylation, we observed that the C−C bond length in the optimized solution-phase geometries of compounds **1** and **7** was essentially unchanged from the typical value (1.54 Å), whereas the C−C bond in the radical cation **10** was lengthened by 0.22 (Figure 2).

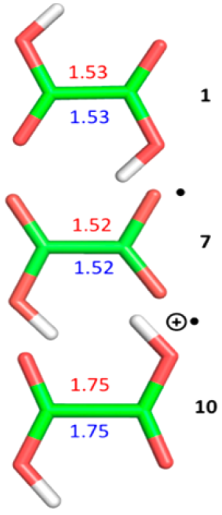

Figure 2. Calculated C−C bond lengths (Å) using CCSD(T)/cc-pVTZ (red) and SMD/M06/cc-pVTZ (blue) descriptions of oxalic acid **1** (top), the neutral radical **7** (middle), and the radical cation **10** (bottom). Color scheme: C, green; H, white; O, red.

Visualization of the singly occupied molecular orbital (SOMO) of **10**, using the Gaussview software package,[24] indeed indicated that the unpaired electron in this radical cation was associated with the C−C σ-bond and contributions from oxygen-based p_x and p_y orbitals (Figure 3). In contrast, the neutral radical exhibited a σ-type SOMO (see Figure S2 in the Supporting Information). To ensure that this observation was not merely an artifact associated with using a Kohn−Sham DFT (KS-DFT) description together with a continuum solvation potential, we computed CCSD(T)/cc-pVTZ structures for **1** and **10** in the gas-phase; such geometries are known

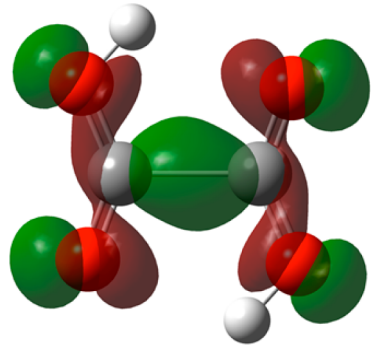

Figure 3. SOMO of the radical cation **10**. The electron density is contoured at 0.06 au, as computed using UHF/cc-pVTZ from the reduced 1-electron density matrix for the radical at the SMD/M06/cc-pVTZ optimized geometry.

to be accurate to within 0.01 Å for single-reference molecules.[25] The C−C bond in **10** was again lengthened (0.22 Å) relative to that in oxalic acid **1** (Figure 2).

The calculated spin-density difference for the ground state of radical cation **10** showed that α-electron density accumulates along the C−C bond and on two oxygen atoms (Figure 4 and Figure S4 in Supporting Information).

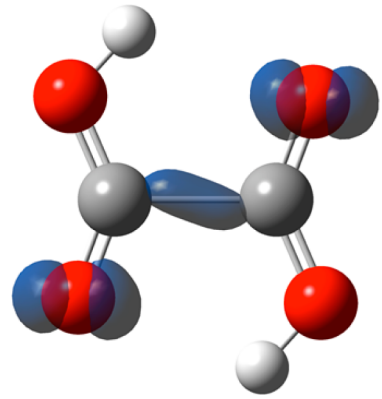

Figure 4. Spin polarization of the radical cation **10**. The excess α electron spin density is contoured at 0.028 au, as computed using UHF/cc-pVTZ from the reduced 1-electron density matrix for the radical at the SMD/M06/cc-pVTZ optimized geometry. Color scheme: C, gray; H, white; O, red.

We also calculated the ionization energies of oxalic acid **1** using ionization potential equation of motion coupled cluster singles and doubles (IP-EOM-CCSD).[13a] IP-EOM-CCSD calculates ionization energies using coupled cluster theory, thereby giving the energetic ordering of the molecular orbitals but with correlation, unlike any ab initio SCF formalism. The calculated IP-EOM-CCSD/cc-pVTZ spectrum for oxalic acid **1** was in excellent agreement with experimental photoelectron spectra[26] (see Table S1 in Supporting Information); the lowest energy IP is associated with a highest occupied molecular orbital (HOMO) of the a_g irreducible representation in C_{2h}. Early work suggested that this ionization corresponds to removing a nonbonding electron from **1**, which presumably is on oxygen.[26] Taken at face value, this could imply an orbital interchange as the C−C bond lengthens. However, after performing IP-EOM-CCSD calculations at longer C−C bond lengths (from 1.53 to1.75 Å; see Table S2 in Supporting Information) the order of the ionization potentials remained

DOI: 10.1021/ja510666r
J. Am. Chem. Soc. 2015, 137, 3248−3252

the same. The bond lengthening does, however, reduce the HOMO ionization potential by 13.6 kcal/mol, which would make it easier to ionize oxalic acid. Visual inspection of the HOMO of oxalic acid **1** (Figure 5) and the SOMO of the radical cation **10** (Figure 3), at their equilibrium geometries, shows them to be quite similar.

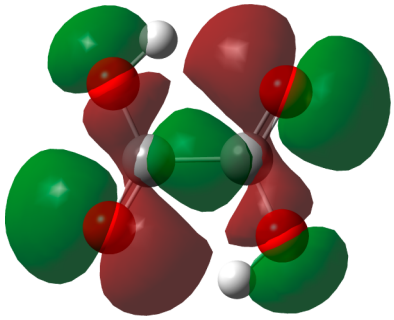

Figure 5. HOMO of oxalic acid **1**. The electron density is contoured at 0.06 au, as computed using UHF/cc-pVTZ from the reduced 1-electron density matrix for the radical at the SMD/M06/cc-pVTZ optimized geometry.

A similar C−C bond lengthening has been calculated for the acetyloxy radical, but this was explained on the basis of orbital phases resulting in nodes.[27]

Single-Electron Bonding and C−C Bond Breaking in Radical Cation 10. In an alternate approach to generate a physical picture of the structural differences observed for the neutral and cationic radicals, we computed the C−C bond orders for **1** (0.88), **7** (0.82), and **10** (0.60).[28] A simple model might be proposed in which there is a "single-electron" C−C σ bond in the radical cation **10** at its equilibrium geometry; consistent with previous literature on odd-electron bonding.[29] The gas-phase bond dissociation energy of a 1 or 3 electron σ bond can be described semiquantitatively by the expression:[29a]

$$D_{AB} = \frac{D_{AA} + D_{BB}}{2} \exp(-\lambda_A \lambda_B |\Delta_{IP}|)$$

where D refers to the bond dissociation energy, A and B are the two fragments of the molecule connected by the 1 (or 3) electron bond, $|\Delta_{IP}|$ refers to the difference in ionization potentials of fragments A and B, and λ is an empirical parameter. The bond dissociation energy will therefore be greatest when $|\Delta_{IP}|$ is zero, i.e. when A and B are identical fragments. Equally, the exponential dependence of D on $|\Delta_{IP}|$ means that the barrier to dissociation will be decreased as the difference in ionization potentials of fragments A and B is increased.[29c] Resonance stabilization of neutral radical **7** requires contributions from ionized resonance structures $[A^{\odot}B^{\odot} \leftrightarrow A^{+}B^{\odot -}]$, which are unimportant compared to that of the uncharged resonance structure. This is not the case for the cation because all resonance structures carry a positive charge $[A^{+\odot}\ B \leftrightarrow AB^{+\odot}]$ and therefore contribute substantially to the actual structure. As a result, the $|\Delta_{IP}|$ for the fragments in the radical cation will be far lower than those of the corresponding neutral radical Δ_{IP}. Hence, qualitatively one would expect that the neutral radical **7** should not, and the radical cation **10** should, have a one-electron σ bond.

CONCLUSIONS

Significant gaps exist in our knowledge of the oxidation and spin states of the metal center during catalytic turnover and exactly how the substrate is coordinated to Mn. These issues preclude QM/MM calculations on the details of the catalytic mechanism, and so our accurate QM studies provide a firm base for future computational investigations into the chemistry that might be employed by OxDC. More specifically, our calculations support the view that the barrier to C−C bond cleavage in oxalic acid is significantly reduced when an electron is removed from the molecule, which is consistent with the idea that the role of the metal in OxDC is to facilitate the removal of an electron from the substrate prior to C−C bond breaking. The relatively low barriers computed for decarboxylation from either of the radical species (**7** or **10**) might also explain why it has proven so difficult to observe any radical intermediates prior to decarboxylation in the OxDC-catalyzed reaction.[3d,21]

COMPUTATIONAL METHODS

KS-DFT calculations were done with the GAMESS software.[14] In general, geometry optimizations used KS-DFT with the M06 functional[7] and cc-pVTZ basis set,[10] in combination with the SMD implicit solvation model for water.[8] Hessians were calculated using finite-difference methods from the analytic gradients. Convergence of the KS reference was given at 10^{-6}, and geometry optimizations were performed until the largest force and RMS force were 3.3×10^{-4} Hartree/Bohr and 1.0×10^{-4} Hartree/Bohr, respectively. The numeric grid used in the KS-DFT calculations consisted of 99 radial and 590 solid-angle points. All computed structures and transition states were confirmed by analysis of the eigenvalues obtained from normal-mode analysis using KS-DFT. Gibbs free energies were calculated from the implicit solvent partition function (M06/cc-pVTZ), solvation energies (M06/cc-pVTZ), and gas-phase, coupled-cluster single point energies (for structures at their "solvated" geometries). All partition functions were scaled using the recommended 0.998 scale factor of Truhlar and co-workers. The latter values corresponded to CCSD(T)/CBS (using a triple-ζ/quadruple-ζ Dunning-based extrapolation).[12] CBS energy values were always within 0.1 kcal/mol of those computed by CCSD(T)/cc-pVQZ.[8] SCF convergence and convergence of the coupled-cluster equations were both achieved at 10^{-6}. All core orbitals were dropped and spherical d functions were used in all basis sets. Harmonic vibrational frequencies were scaled by a factor of 0.998.[30]

Calculations to confirm the geometric properties of the doublet cation **10** were performed using CCSD(T)/cc-pVTZ optimization (gas phase), as implemented in the ACES2 software package.[15] Convergence of the reference wave functions for both doublet species **7** and **10** proved nontrivial (see Supporting Information); in particular, the converged restricted openshell Hartree-Fock density often had to be used as the initial guess for the unrestricted Hartree-Fock reference wave function.

ASSOCIATED CONTENT

Supporting Information

Absolute energies, harmonic vibrational frequencies, and coordinates for structures **1**−**12**, energetic values for the decarboxylation of alternate rotamers of oxalic acid **1** and the radical cation **10**, figures showing the SOMO and spin polarization of the neutral radical **7**, the IP-EOM-CCSD energies computed for oxalic acid **1**, and an alternate version of Figure 4; complete ref 15. This material is available free of charge via the Internet at http://pubs.acs.org.

AUTHOR INFORMATION

Corresponding Author

ngrichar@iupui.edu

DOI: 10.1021/ja510666r
J. Am. Chem. Soc. 2015, 137, 3248−3252

Notes

The authors declare no competing financial interest.

■ ACKNOWLEDGMENTS

We thank the University of Florida (UF) for provision of an Alumni Fellowship (A.M.L.). We also acknowledge Dr. Ajith Perera (Quantum Theory Project, UF) and Prof. John Stanton (Texas) for providing useful insights into SCF convergence and the technical difficulties associated with calculating the properties of the neutral doublet 7, respectively. These studies were funded by the National Institutes of Health (DK061666 to N.G.J.R.) and the Army Research Office (US.ARO.W911NF-12-1-0143 to R.J.B). Computing resources for this project were provided by the UF High Performance Computing Center and the IUPUI School of Science.

■ REFERENCES

(1) (a) Svedruzic, D.; Jonsson, S.; Toyota, C. G.; Reinhardt, L. A.; Ricagno, S.; Lindqvist, Y.; Richards, N. G. J. *Arch. Biochem. Biophys.* **2005**, *413*, 176−192. (b) Tanner, A.; Bornemann, S. *J. Bacteriol.* **2000**, *182*, 5271−5273. (c) Mehta, A.; Datta, A. *J. Biol. Chem.* **1991**, *266*, 23548−23553. (d) Lillehoj, E. B.; Smith, F. G. *Arch. Biochem. Biophys.* **1965**, *109*, 216−220. (e) Emiliani, E.; Bekes, P. *Arch. Biochem. Biophys.* **1964**, *105*, 488−493. (f) Shimazono, H.; Haiyashi, O. *J. Biol. Chem.* **1957**, *227*, 151−159.

(2) (a) Costa, T.; Steil, L.; Martins, L. O.; Volker, U.; Henriques, A. O. *J. Bacteriol.* **2004**, *186*, 1462−1474. (b) Walz, A.; Zingen-Sell, I.; Theisen, S.; Kortekamp, A. *Eur. J. Plant Pathol.* **2008**, *120*, 317−330.

(3) (a) Reinhardt, L. A.; Svedruzic, D.; Chang, C. H.; Cleland, W. W.; Richards, N. G. J. *J. Am. Chem. Soc.* **2003**, *125*, 1244−1252. (b) Svedruzic, D.; Liu, Y.; Reinhardt, L. A.; Wroclawska, E.; Cleland, W. W.; Richards, N. G. J. *Arch. Biochem. Biophys.* **2007**, *464*, 36−47. (c) Saylor, B. T.; Reinhardt, L. A.; Lu, Z.; Shukla, M. S.; Nguyen, L.; Cleland, W. W.; Angerhofer, A.; Allen, K. N.; Richards, N. G. J. *Biochemistry* **2012**, *51*, 2911−2920. (d) Imaram, W.; Saylor, B. T.; Centonze, C.; Richards, N. G. J.; Angerhofer, A. *Free Radical Biol. Med.* **2011**, *50*, 1009−1015.

(4) Yuan, Y.; Wolfenden, R.; Lewis, C. A. *J. Am. Chem. Soc.* **2011**, *133*, 5683−5685.

(5) Burrell, M. R.; Just, V. J.; Bowater, L.; Fairhurst, S. A.; Requena, L.; Lawson, D. M.; Bornemann, S. *Biochemistry* **2007**, *46*, 12327−12336.

(6) (a) van der Kamp, M. W.; Mulholland, A. J. *Biochemistry* **2013**, *52*, 2708−2728. (b) Lonsdale, R.; Harvey, J. N.; Mulholland, A. J. *Chem. Soc. Rev.* **2012**, *41*, 3025−3038.

(7) (a) Blomberg, M. R. A.; Borowski, T.; Himo, F.; Liao, R.-Z.; Siegbahn, P. E. M. *Chem. Rev.* **2014**, *114*, 3601−3658. (b) Siegbahn, P. E. M.; Himo, F. *J. Biol. Inorg. Chem.* **2009**, *14*, 643−651.

(8) Truhlar, D. G.; Marenich, A. V.; Cramer, C. J. *J. Phys. Chem. B* **2009**, *113*, 6378−6396.

(9) Zhao, Y.; Truhlar, D. G. *Theor. Chem. Acc.* **2008**, *120*, 215−241.

(10) Dunning, T. H. *J. Chem. Phys.* **1989**, *90*, 1007−1023.

(11) (a) Marenich, A. V.; Ding, W.; Cramer, C. J.; Truhlar, D. G. *J. Phys. Chem. Lett.* **2012**, *3*, 1437−1442. (b) Ribeiro, R. F.; Marenich, A. V.; Cramer, C. J.; Truhlar, D. G. *J. Comput.-Aided. Mol. Des.* **2010**, *24*, 317−333. (c) Truhlar, D. G.; Marenich, A. V.; Cramer, C. J.; Truhlar, D. G. *J. Phys. Chem. B* **2009**, *113*, 4538−4543.

(12) Bak, K. L.; Jørgensen, P.; Olsen, J.; Helgaker, T.; Klopper, W. *J. Chem. Phys.* **2000**, *112*, 9229−9242.

(13) (a) Bartlett, R. J.; Musial, M. *Rev. Mod. Phys.* **2007**, *79*, 291−352. (b) Pople, J. A.; Head-Gordon, M.; Raghavachari, K. *J. Chem. Phys.* **1987**, *87*, 5968−5975. (c) Urban, M.; Noga, J.; Cole, S.; Bartlett, R. J. *J. Chem. Phys.* **1985**, *83*, 4041−4047.

(14) Schmidt, M. W.; Baldridge, K. K.; Boatz, J. A.; Elbert, S. T.; Gordon, M. S.; Jensen, J. H.; Koseki, S.; Matsunaga, N.; Nguyen, K. A.; Su, S. J.; Windus, T. L.; Dupuis, M.; Montgomery, J. A. *J. Comput. Chem.* **1993**, *14*, 1347−1363.

(15) Stanton, J. F.; Gauss, J. et al.. *ACES2*; University of Florida, Gainesville, FL, 2006.

(16) Lotrich, V.; Flocke, N.; Ponton, M.; Yau, A. D.; Perera, A.; Deumens, E.; Bartlett, R. J. *J. Chem. Phys.* **2008**, *128*, 194104.

(17) (a) Schreiner, P. R.; Reisenauer, H. P. *Angew. Chem., Int. Ed.* **2008**, *47*, 7071−7074. (b) Chang, J.-G.; Chen, H.-T.; Xu, S.; Lin, M. C. *J. Phys. Chem. A* **2007**, *111*, 6789−6797. (c) Higgins, J.; Zhou, X.; Liu, R. F.; Huang, T. T.-S. *J. Phys. Chem. A* **1997**, *101*, 2702−2708.

(18) Information on the relative energetics, free energy barriers, *xyz* coordinates, and harmonic vibrational frequencies for the full set of alternate rotamers is available from the authors upon request.

(19) Yanai, T.; Tew, D. P.; Handy, N. C. *Chem. Phys. Lett.* **2004**, *393*, 51−57.

(20) Peverati, R.; Truhlar, D. G. *J. Phys. Chem. Lett.* **2011**, *2*, 2810−2817.

(21) Chang, C. H.; Svedruzic, D.; Ozarowski, A.; Walker, L.; Yeagle, G.; Britt, R. D.; Angerhofer, A.; Richards, N. G. J. *J. Biol. Chem.* **2004**, *279*, 52840−52849.

(22) (a) Chatgilialoglu, C.; Crich, D.; Komatsu, M.; Ryu, I. *Chem. Rev.* **1999**, *99*, 1992−2069. (b) Costentin, C.; Robert, M.; Saveant, J. M. *J. Am. Chem. Soc.* **2003**, *125*, 105−112. (c) Bucher, G.; Halupka, M.; Kolano, C.; Schade, O.; Sander, W. *Eur. J. Org. Chem.* **2001**, 545−552. (d) Poad, B. L. J.; Kirk, B. B.; Hettiarachchi, P. I.; Trevit, A. J.; Blanksby, S. J.; Clark, T. *Angew. Chem., Int. Ed.* **2013**, *52*, 9301−9304. (e) Ryzhkov, L. R. *J. Org. Chem.* **1996**, *61*, 2801−2808. (f) Feller, D.; Huyser, E. S.; Borden, W. T.; Davidson, E. R. *J. Am. Chem. Soc.* **1983**, *105*, 1459−1466.

(23) Andrieux, C. P.; Gonzalez, F.; Saveant, J. M. *J. Electroanalyt. Chem.* **2001**, *498*, 171−180.

(24) Dennington, R.; Keith, T.; Millam, J. *GaussView*, version 5, Semichem Inc.: Shawnee Mission, KS, 2009.

(25) Helgaker, T.; Gauss, J.; Jørgenson, P.; Olsen, J. *Chem. Phys.* **1997**, *106*, 6430−6440.

(26) Meeks, J. L.; Arnett, J. F.; Larson, D. B.; McGlynn, S. P. *J. Am. Chem. Soc.* **1975**, *97*, 3905−3908.

(27) Rauk, A.; Yu, D.; Armstrong, D. A. *J. Am. Chem. Soc.* **1994**, *116*, 8222−8228.

(28) Mayer, I. *J. Comput. Chem.* **2007**, *28*, 204−221.

(29) (a) Clark, T. *J. Am. Chem. Soc.* **1988**, *110*, 1672−1678. (b) Hiberty, P. C.; Humbel, S.; Danovich, D.; Shaik, S. *J. Am. Chem. Soc.* **1995**, *117*, 9003−9011. (c) Clark, T. Ab initio Calculations on Electron-Transfer Catalysis by Metal Ions. In *Topics in Current Chemistry*; Mattay, J., Ed.; Springer Verlag: Heidelberg, Germany, 1996; Vol. *77*; pp 1−24.

(30) Alecu, I. M.; Zheng, J.; Zhao, Y.; Truhlar, D. G. *J. Chem. Theory Comput.* **2010**, *6*, 2872−2887.

DOI: 10.1021/ja510666r
J. Am. Chem. Soc. 2015, 137, 3248−3252